

Early age microstructure of Portland cement mortar investigated by ultrasonic shear waves and numerical simulation

Thomas Voigt^{a,*}, Guang Ye^b, Zhihui Sun^a, Surendra P. Shah^a, Klaas van Breugel^c

^aNorthwestern University, Center for Advanced Cement-Based Materials, 2145 Sheridan Road, Suite A130, Evanston, IL 60208, USA

^bGhent University, Department of Structural Engineering, Magnel Laboratory for Concrete Research, Technologiepark-Zwijnaarde 904, 9052 Ghent (Zwijnaarde), Belgium

^cDelft University of Technology, Faculty of Civil Engineering and Geosciences, P.O. Box 5048, 2600 GA Delft, The Netherlands

Received 18 February 2004; accepted 7 September 2004

Abstract

This paper investigates the ability of a shear wave reflection (WR) method to monitor microstructural changes of Portland cement mortar during hydration. The wave reflection method measures the reflection loss of shear waves at an interface between a steel plate and mortar. Mortars with water/cement ratios of 0.35, 0.5 and 0.6 were tested at isothermal curing conditions of 25 °C. The numerical model HYMOSTRUC3D was used to simulate the evolution of microstructural properties of the cement paste phase of the tested mortars. The parameters obtained from the simulations were the volume fraction of the total and connected solid phase and the specific contact area of the hydrated cement particles. The investigations have shown that the wave reflection measurements are governed primarily by the degree of the inter-particle bonding of the cement particles as calculated from the specific contact area of a simulated microstructure.

© 2004 Elsevier Ltd. All rights reserved.

Keywords: Hydration; Microstructure; No category: nondestructive testing; Numerical simulation

1. Introduction

A very significant portion of today's civil infrastructure is partially or completely made out of cementitious materials. The constantly increasing expectations to the performance of this infrastructure call for quality control measures to assure healthy and durable buildings. Repeated failures of concrete structures at early ages have shown that this is one of the most critical periods of the life time of this construction material and that the availability of information about early age concrete is most essential. A relatively large variety of methods is available to provide information about early age concrete properties. The principle of these methods consists of measuring certain parameters (e.g., mechanical, electrical, or acoustical) and

then relating these parameters to the desired concrete properties by using empirical relationships. This often requires advance calibration or the application of complementary methods.

The research described in this paper has the objective to overcome this practice and to develop a method that allows the description of the physical parameters of concrete as a result of its true microstructure rather than relying on empirical laws. An ultrasonic wave reflection (WR) technique based on high frequency shear waves has been developed recently [1,2]. The method measures the reflection coefficient of ultrasonic waves at the interface of a buffer material and hydrating cementitious materials. Previous investigations have shown that the wave reflection (WR) method has a high sensitivity to the progress of the hydration of cementitious materials. The differences in the hydration rate caused by factors such as retarding or accelerating admixtures can be detected reliably [1,2]. The experiments have also proven that the WR method is able to

* Corresponding author. Tel.: +1 847 467 3630; fax: +1 847 467 1078.

E-mail address: th-voigt@northwestern.edu (T. Voigt).

follow the development of parameters such as compressive strength, elastic moduli and degree of hydration [3–6]. This paper describes investigations that detail the relationship between the wave reflection measurements and microstructural changes in cementitious materials occurring during the course of hydration. Thermogravimetry (TG) is used to experimentally assess physico-chemical parameters of the tested materials.

In the recent years several microstructural and micro-mechanical models for the evolution of the microstructure of hydrating cementitious materials have been developed [7–13]. These models allow to effectively assess the properties of cement-based materials based on their composition and curing history. The described research has employed such a numerical model (HYMOSTRUC [7]) to simulate the microstructure of Portland cement. The numerical modeling is used as an effective tool to link the ultrasonic measurements with parameters of the cementitious microstructure. The ultimate objective of the research presented here is to develop a sensor based on the WR technique that has the ability to read the information stored in the cementitious nano- and microstructure and to immediately use this data to infer its mechanical properties.

2. Experimental program

2.1. Materials

Portland cement mortars with different water/cement (w/c) ratios (0.35, 0.5, 0.6) were investigated in this study. Portland cement type I and silica sand as fine aggregates were used as the mixture ingredients in a mass ratio of cement/sand=1:2. The mortars were cured at isothermal conditions at 25 °C throughout the duration of the experiments. Some experiments and the numerical simulations described in the following were conducted with cement paste of the same w/c ratios as used for the mortars. Since the tested mortars contain pure silica sand, which does not have any water absorption, the hydration behavior of paste and mortar with the same w/c ratio can be considered as identical. Hence, for a given w/c ratio any parameter

measured or calculated for the cement paste can be used to describe the appropriate properties of the cement paste phase of the mortar.

2.2. Wave reflection method

To investigate the hydration behavior of the cement mortars, the wave reflection method was applied. The wave reflection method monitors the reflection loss of ultrasonic shear waves at an interface between a steel plate and a cementitious material over time. The amount of the lost wave amplitude depends on the reflection coefficient, which in turn is a function of the acoustical properties of the materials that form the interface.

A schematic of this experimental technique is shown in Fig. 1. A steel plate is brought in contact with fresh mortar. And a transducer with a frequency of 2.25 MHz, which is attached to the steel plate, transmits a shear wave pulse into the steel. When the mortar is in liquid state the pulse is entirely reflected at the steel/mortar interface, since shear waves do not propagate in liquid materials (Fig. 1a). Thus, the reflection coefficient is unity. With proceeding hydration the cement grains percolate and build up a skeleton allowing the shear waves to propagate. This allows the shear waves to pass the interface resulting in reflection losses during the reflection process (Fig. 1b). Consequently, the reflection coefficient starts to decrease. With proceeding hydration the ability of the cement mortar to transmit shear waves gains higher levels. More and more wave energy is transmitted into the cement paste and the reflection coefficient decreases further. After a certain time this process decelerates and the reflection coefficient approaches a final value. At this time changes in the microstructure of the cement mortar due to hydration are too small to alter the shear wave propagation properties significantly.

The reflection coefficient r is calculated from the ratio of the amplitudes of the first (A_1) and second reflections (A_2) received from the steel/mortar interface (Eq. (1)). A detailed explanation of the calculation of the reflection coefficient can be found elsewhere [1,2]. Basically, the reflection coefficient represents an amplitude ratio and describes the relative loss in amplitude between the first and second

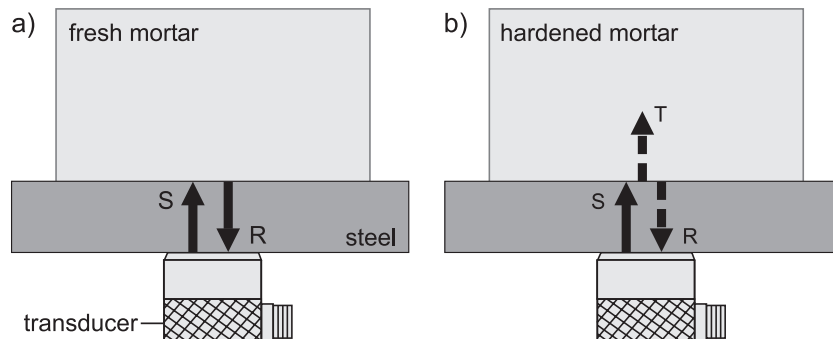


Fig. 1. Principle of wave reflection method.

reflection at a given time t . In ultrasonics, amplitude ratios are usually measured in decibel. The reflection coefficient $r(t)$ expressed in decibel becomes the reflection loss $R_L(t)$. The conversion of r into R_L can be done with Eq. (2) with $R_L(t)$ as the reflection loss at time t and $r(t)$ as the reflection coefficient at time t .

$$r = \frac{A_2}{A_1} \quad (1)$$

$$R_L(t) = -20 \log(r(t)) \quad (2)$$

2.3. Thermogravimetry

Thermogravimetry (TG) has been used frequently for studying the hydration of Portland cements, by considering the fact that the hydration reaction between the mixing water and cement can be reversed when the hardened cement paste is subjected to high temperatures [14,15]. TG measurements of cement paste were performed in order to determine the amount of the evaporable and non-evaporable water in the hydrating cement paste. Samples of approximately 150 mg were taken by crushing cubes of cement paste that were cast in common ice cube trays. The TG was performed immediately after the sampling process. The cement paste was cured at isothermal conditions (25 °C) and the measurements started as early as 1 h after casting. The samples were heated up to a temperature of 900 °C according to a defined heating regime. During the heating process the sample loses weight due to the evaporation of the free and the decomposition of the chemically combined water. In order to distinguish between evaporable and non-evaporable water, the temperature was first increased to 105 °C, held at that value for 2 h and then increased further to 900 °C. The heating rate was 10 °C/min. The samples were heated in a steady flow of dry, CO₂-free nitrogen. The result of the TG is the development of the weight loss of the sample during heating. More details on the heating regime and the results of the TG measurements are given in Ref. [5].

Two parameters, the amount of the total water and the non-evaporable water in the cement paste, can be derived directly from TG measurements. The difference between the initial sample weight (m_0) and the weight at 900 °C (m_{900}) yields the amount of the total water (w_t) held in the cement paste at the time of testing. The amount of the total water needs to be corrected by the weight loss of the dry cement powder at 900 °C with respect to its initial mass ($L_{0/900}$). The amount of non-evaporable water (w_n) is calculated from the weight loss measured between 105 and 900 °C corrected by the loss of ignition of the dry cement powder at 900 °C with respect to its mass at 105 °C ($L_{105/900}$). The amounts of the two types of water are expressed in gram per gram of original cement. The equations for calculating the content of the total water (w_t/c) and non-evaporable water per gram of original cement (w_n/c) are given in Eqs. (3) and (4), respectively. If both quantities are known, the amount of the evaporable

water per gram of original cement can be calculated with Eq. (5). The calculation of the non-evaporable water from the weight loss of cement paste after heating was first derived by Powers [16].

$$\frac{w_t}{c} = \frac{m_0}{m_{900}} (1 - L_{0/900}) - 1 \quad (3)$$

$$\frac{w_n}{c} = \frac{m_{105}}{m_{900}} (1 - L_{105/900}) - 1 \quad (4)$$

$$\frac{w_e}{c} = \frac{w_t}{c} - \frac{w_n}{c} \quad (5)$$

The amount of non-evaporable water is commonly considered as an approximation of the chemically bound water, although much water from the interlayer spaces, which is by definition part of the chemically bound water, is lost during the drying process at 105 °C [17, pp. 120–121]. Thus, by relating the content of non-evaporable water at a certain time t to that for complete hydration, the degree of hydration can be calculated. The content of non-evaporable water for complete hydration (w_n/c_{complete}) was determined based on the maximum water content of the clinker phases of the used cement as it can be found in the literature [18]. The value obtained from this calculation ($w_n/c_{\text{complete}} = 0.236$) corresponds well with that given by Taylor [17, p. 198] as typical for fully hydrated Portland cement pastes ($w_n/c_{\text{complete}} = 0.23$).

$$w_g = a k w_n \quad (6)$$

The amount of the evaporable water (Eq. (5)) equals the sum of the mass of the capillary and the gel water held in the cement paste. To distinguish between capillary and gel water, a relation derived from the Powers–Brownyard model for the structure of hardened Portland cement paste was used. In Eq. (6) the weight of the gel water (w_g) is defined as a fraction of the non-evaporable water (w_n). The parameters a and k , which were originally derived from water absorption studies on cement paste at different vapor pressures, are taken from the literature [19]. The parameters can be considered to be constant with $a=3.3$ and $k=0.25$. Since the cement paste was cured at saturated conditions, it will be assumed that all capillary pores were filled with water. This justifies that the mass of the capillary water determined with the TG measurements can be used to determine the capillary porosity.

3. Numerical simulation

3.1. General principle and output parameters

A numerical model, HYMOSTRUC3D, was developed to allow the simulation of the hydration process of Portland cement [7,8]. In this model, the degree of hydration is simulated as a function of the particle size distribution and

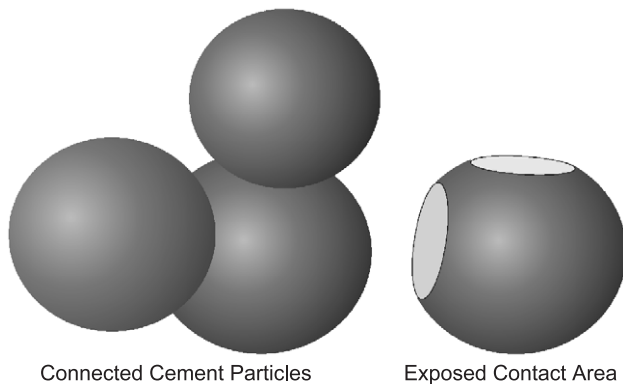


Fig. 2. Contact area of cement particles.

of the chemical composition of the cement, the w/c ratio and the reaction temperature. HYMOSTRUC3D models the hydrating cement particles as growing spheres randomly distributed in a cubic 3D body (side length 100 μm). As cement hydrates, the cement grains gradually react and a porous shell of hydration products is formed around the grain. This results in an outward growth or “expansion” of the particles. As hydration progresses, the growing particles become more and more connected. The material evolves from the state of a suspension to the state of a porous elastic solid.

HYMOSTRUC3D assumes that the microstructure of hydrating cement paste consists of two major phases: the solid and the pore phase. The solid phase is formed by the hydration products and the unhydrated cement. The pore phase comprises capillary pores that are filled with air or water. By applying a serial section concept, associated with an overlap criterion [12], the numerical model allows the calculation of various parameters that describe the properties of these two phases during the hydration of the cement. Within the scope of this paper, parameters characterizing the volumetric distribution and the connectivity of the phases will be used. The following output parameters of the model will be analyzed:

- volume fraction of the total solid and pore phase
- volume fraction of connected solid phase
- percolation threshold of solid phase
- specific contact area of cement particles.

The volume fraction of the phases gives the relative volume of the 3D body that is occupied by the solid or pore phase at a certain hydration time. The initial value of this parameter depends solely on the w/c ratio of the simulated cement paste. The volume fraction of the connected solid phase represents the relative volume of the 3D body that is occupied by solid particles that are continuously connected and thereby providing an uninterrupted link between two opposite faces of the 3D body. The volume fraction of the solid phase at which the solid starts to become interconnected from one side to another is defined as the

percolation threshold of the solid phase. The time when the percolation threshold occurs is defined as percolation time. While the volume fraction of the connected solid phase yields information only about the amount of the connected solid, it would be desirable to have a parameter available that describes the degree of the inter-particle bonding.

The contact area of the solid phase can provide such a measure. If a cluster of connected solid particles is considered (Fig. 2a), the contact area for this cluster is the sum of the areas that establish the connection between the individual particles (Fig. 2b). HYMOSTRUC3D computes the specific contact area of the hydrated cement particles, which is defined as the contact area per unit volume of cement paste at a given hydration age.

3.2. Calibration of the model

An important requirement for the use of numerical simulations is information about the reliability of the obtained results. To assure that the simulation results are comparable to the actual experiments, the numerical model has to be calibrated. For the presented study the model was calibrated in two ways. The first calibration parameter is the particle size distribution (PSD) of the cement that was used in the conducted experiments. The PSD of the dry cement powder was determined experimentally and then used to adjust the HYMOSTRUC3D program. A comparison between the PSD determined by experiment and that calculated by HYMOSTRUC3D is shown in Fig. 3.

A second way of calibration was to compare the degree of hydration calculated by HYMOSTRUC3D with the degree of hydration determined by experiments. The parameters that determine the kinetics of the cement hydration simulated by HYMOSTRUC3D were adjusted until the simulated and experimental values were brought to an acceptable agreement. Based on the described calibrations of the model to conducted experiments, the results obtained from the numerical model can be considered to be valid and reliable.

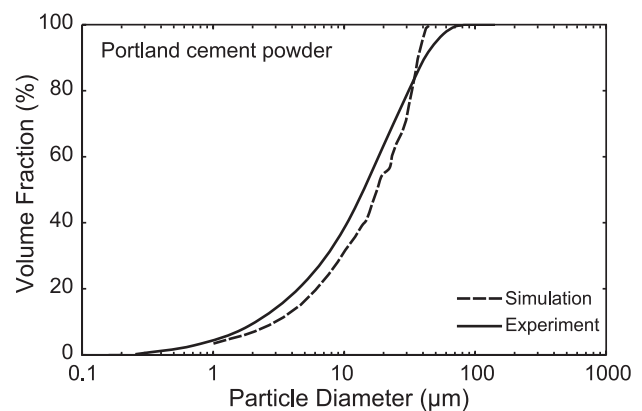


Fig. 3. Comparison between the particle size distributions determined by experiments and calculated by HYMOSTRUC3D.

4. Results and discussion

4.1. Reflection loss, degree of hydration and capillary porosity

The relationship between the reflection loss of the three tested mortar mixtures and the degree of hydration of the cement paste phase of the mortars is given in Fig. 4. The degree of hydration was determined from the amount of the non-evaporable water measured by TG. As it can be seen from the figure, for each mortar mixture, the presented data show a very strong linear trend over the entire period of time that is plotted. The coefficients of determination, R^2 , of the plotted trend lines are given in the figure to illustrate the statistical significance of the trends. By comparing the relationships of the different w/c ratios, it is obvious that the slope of the relationship changes with the w/c ratio, where a low w/c ratio corresponds to a steep slope. In other words, for a given degree of hydration, the reflection loss of the mortar with w/c=0.35 is higher than the reflection loss of the mortar with, e.g., w/c=0.6.

This indicates that the reflection loss is not only a function of the progress in hydration but also a measure of microstructural properties as influenced, for example, by the w/c ratio. It was observed that the three trends given in Fig. 4 can be transformed into a unique relationship by relating the reflection loss of the mortars to the gel-space ratio of the cement paste phase of the tested mortars. Since the gel-space ratio describes the characteristics of the capillary porosity, it can be assumed that the latter parameter has a significant influence on the evolution of the reflection loss.

The relationship between the reflection loss and the capillary porosity for the tested mortar mixtures is given in Fig. 5. The capillary porosity was determined from the mass of the capillary water in the cement pastes measured by TG. For all three w/c ratios it can be stated that the reflection loss strongly depends on the development of the capillary porosity. A decrease of the capillary porosity due to hydration is followed by a steep increase of the reflection

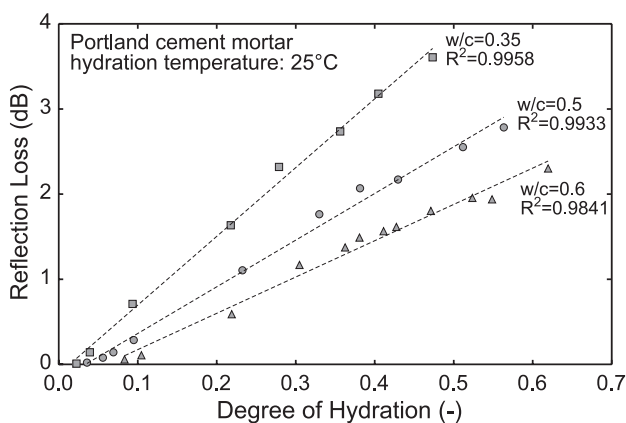


Fig. 4. Relationship between reflection loss and degree of hydration for tested cement mortars.

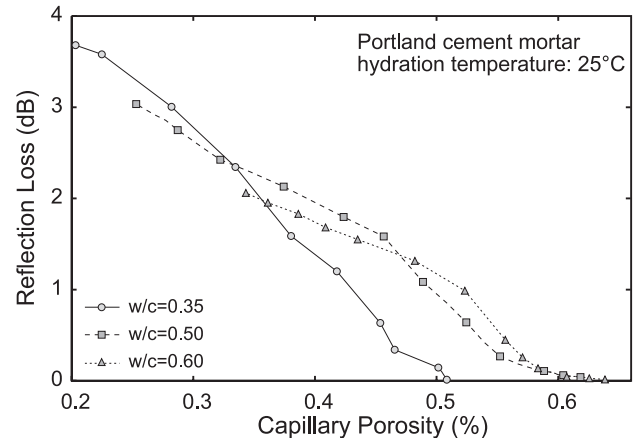


Fig. 5. Relationship between reflection loss and capillary porosity for tested cement mortars.

loss. Except for very high porosities for w/c=0.5 and 0.6 the presented relationships are dominated by a linear pattern. The horizontal shift of the three graphs originates from the different initial values of the capillary porosity caused by the w/c ratio. This example shows vividly how the reflection loss measured on the composite of cement paste and sand is affected by the properties of the cement paste phase. The densification of the microstructure caused by the occupation of capillary pore space with hydration products improves the ability of the cement paste to transmit ultrasonic shear waves and thereby causes the measured reflection loss to increase. A similar relationship between the reflection loss and the relative decrease of the capillary porosity of cement pastes with different w/c ratios was reported by Sun et al. [20].

4.2. Reflection loss and volume fraction of the solid phase

In this section, it will be investigated how the microstructural parameters obtained from the numerical simulations with HYMOSTRUC3D can be used to explain the behavior of the experimentally determined reflection loss. The first parameters obtained from numerical simulation that should be compared to the reflection loss measurements are the volume fractions of the total and the connected solid phase. The evolution of these two parameters in time for the cement pastes with w/c=0.35 and 0.6 is given in Fig. 6. The initial value for the volume fraction of the total solid phase S_t is determined by the w/c ratio. Except for the difference in the initial value that causes a vertical shift between the two curves, no other significant influence of the w/c ratio can be identified in the further evolution of parameter S_t . Both curves develop after the same pattern.

The development of the volume fraction of the connected solid phase S_c is much more influenced by the w/c ratio. The first difference is the time of increase of the curve, which marks the time of the percolation threshold t_p . As shown in Fig. 6 the percolation threshold of the solid phase for the paste with w/c=0.6 occurs more than 3 h later compared to the paste with w/c=0.35. Another characteristic influenced

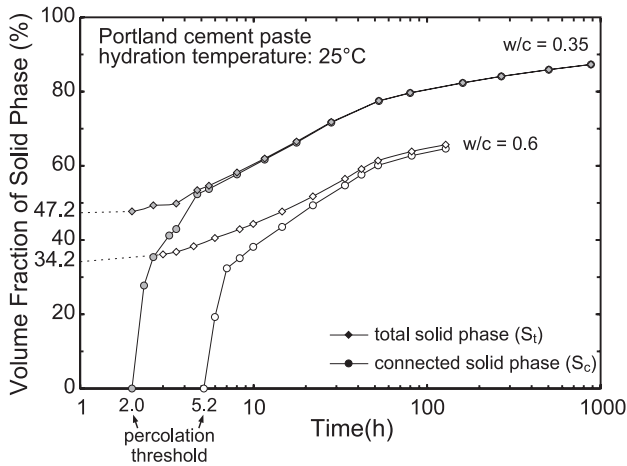


Fig. 6. Volume fraction and percolation threshold of the solid phase for the cement pastes with $w/c=0.35$ and 0.6 as simulated with HYMOSTRUC3D.

by the w/c ratio is how fast the values of the connected solid phase approach those of the total solid phase. The parameters S_t and S_c for $w/c=0.35$ have very similar values after only 5 h and thereafter the change in the difference between the two parameters is very small. On the contrary, the difference between S_t and S_c for $w/c=0.6$ remains large for a significantly longer time. Both values start to develop after a parallel trend after about 50 h.

In Fig. 6 it was shown that the volume fraction of the total and connected solid phase can be used to identify differences in the hydration kinetics and the microstructural development of cement pastes of different compositions. It will now be investigated if the trends found for the parameters S_t and S_c can be used to explain the development of the reflection loss measured on cement mortars prepared with the appropriate w/c ratios. The comparison between the reflection loss and the parameters S_t and S_c in time for the different w/c ratios is given in Figs. 7a–c. Additionally, the ratio of the volume fraction of total to connected solid phase is given in part b of each figure. This ratio will be used to further characterize the development of the connected solid phase.

From the three figures it can be seen that the time of the percolation threshold and the time of increase of the reflection loss are very similar for all three tested w/c ratios. This indicates that the initial stage of the reflection loss development is governed by the connectivity of the cement particles. This assumption seems reasonable since the ability of the cement paste to transmit shear waves, which in turn governs the reflection loss, requires a shear-rigid microstructure that can only be created by interconnected solid particles. A similar relationship between the shear wave reflection coefficient and the percolation threshold of reactive powder concrete was reported by Feylessoufi et al. [21]. In this study, the time of the initial decrease of the shear wave reflection coefficient was found to be related to the time of the percolation threshold, determined by chemical shrinkage measurements.

After the occurrence of the percolation threshold, the volume fraction of the connected solid phase increases rapidly, which results in a steep rise of the reflection loss. The creation of additional inter-particle bonds during this time obviously improves the shear wave propagation properties of the material, further causing the reflection loss to increase.

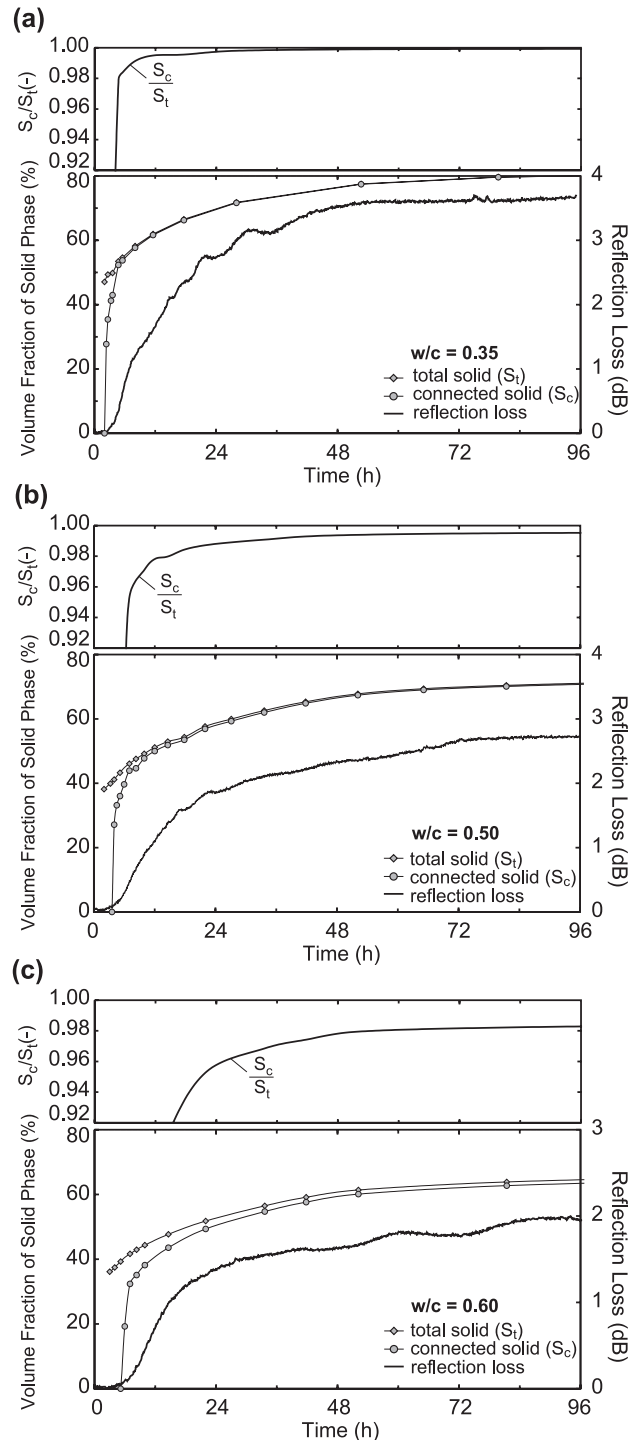


Fig. 7. Comparison of reflection loss and volume fraction of total solid and connected solid phase for mortar/cement paste with (a) $w/c=0.35$, (b) $w/c=0.5$, and (c) $w/c=0.6$.

Based on this characterization of the volume fraction of the solid phase, the development of the reflection loss can be evaluated accordingly. The initial development of the reflection loss is governed by the evolution of the connected solid phase and is characterized by a steep increase. The development of the reflection loss at the later age follows that of the total solid phase and is represented by a moderate or low growth rate. In general, the transition between the two stages occurs at approximately the same time when the difference between connected and total solid phase approaches a constant value. To allow a better evaluation of the change of the connected solid phase relative to the total solid phase, the ratio between both parameters is plotted in the upper part of each subfigure. If, on a qualitative basis, the development of this ratio is compared to that of the reflection loss, it can be found that the smaller the change of ratio S_c/S_t , the smaller also is the change of the reflection loss.

4.3. Reflection loss and specific contact area

In the previous section it was shown that the evolution of the reflection loss measured on mortar mixtures can be explained based on the development of the volume fraction of the total and connected solid phase of cement paste with the same w/c ratio. However, a general relationship, valid independently from the composition of the cement pastes, could not be formulated. In the following it is presented how the previously introduced specific contact area of the cement particles can be used to describe the wave reflection measurements of cementitious materials in a more unique manner.

The relationship between the specific contact area and the degree of hydration for the different cement pastes is given in Fig. 8. For any given degree of hydration, the specific contact area is larger for smaller w/c ratios. This can be attributed to the higher volume of cement contained in those mixtures. It should also be noted that the rate at which

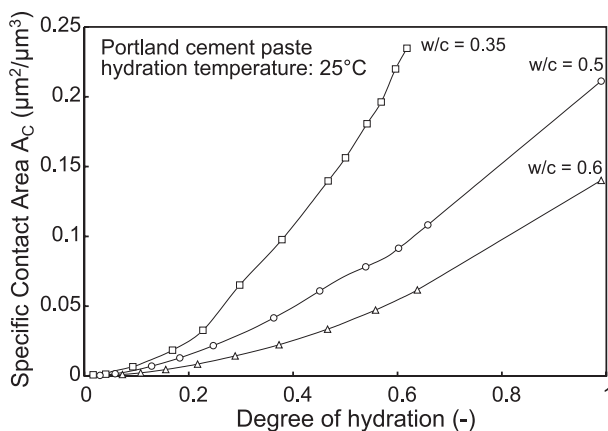


Fig. 8. Relationship between specific contact area and degree of hydration for the tested cement pastes.

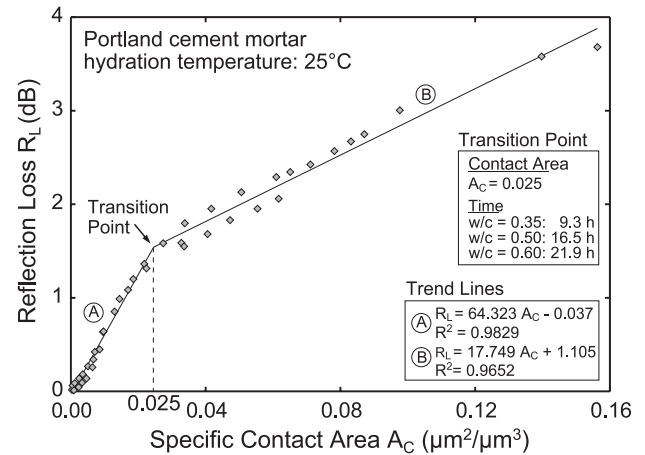


Fig. 9. Relationship between reflection loss (mortar) and specific contact area (cement paste).

the specific contact area increases is higher for the pastes with low w/c ratios. Considering these characteristics, it can be concluded that the development of the specific contact area of the three cement pastes shown in Fig. 8 exhibits the same patterns as the development of the reflection loss vs. the degree of hydration given in Fig. 4. This suggests to further investigate how reflection loss and specific contact area are related.

In Fig. 9 the relationship between these parameters is plotted, where the reflection loss was measured on mortars and the specific contact area refers to cement paste. It can be seen that the reflection loss and the specific contact area of all three tested w/c ratios have a unique bilinear relationship. The trend line describing the early age behavior (Trend A in Fig. 9) can be considered to pass through the origin. This indicates that the reflection loss directly depends on the specific contact area during this time, since no reflection loss can be measured when no contacts between cement particles have been created and the specific contact area is zero. This behavior shows differences compared to the relationship between the reflection loss and the percolation threshold shown in Fig. 7a–c. These figures show that the reflection loss already starts to increase slightly before the occurrence of the percolation threshold.

The initial trend changes its slope after a certain value of reflection loss or specific contact area is reached. The time of this transition is different for the different w/c ratios and is given in Fig. 9. The trend lines A and B have a high statistical significance expressed by their coefficients of determination R^2 , which are also given in Fig. 9. Based on these observations, it can be concluded that the reflection loss is strongly correlated with the specific contact area. This implies that the wave reflection technique is not only sensitive to the volume of the connected solid particles as concluded in the previous section, but also a measure of the degree of the inter-particle bonding in the cementitious microstructure.

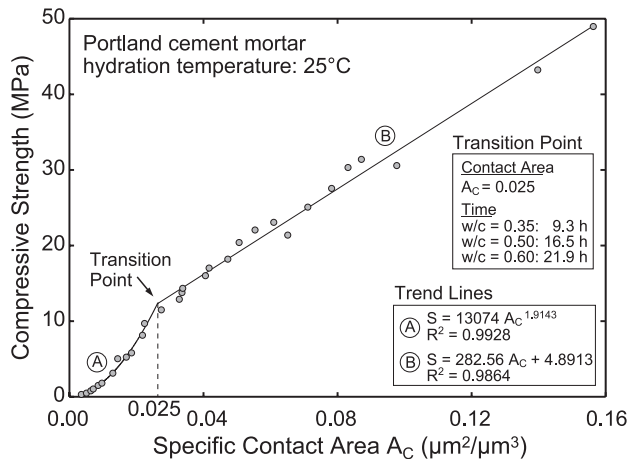


Fig. 10. Relationship between compressive strength (mortar) and specific contact area (cement paste).

4.4. Specific contact area and compressive strength

To evaluate the potential of the specific contact area to explain the evolution of other properties of cementitious materials, its relationship to the compressive strength will be investigated in this section. The compressive strength was determined on mortar mixtures with the three w/c ratios according to ASTM-Standard C 109 [22]. The relationship between the specific contact area and the compressive strength is given in Fig. 10.

It can be seen from the figure that also the compressive strength has a very unique relationship to the specific contact area. Similar to the reflection loss, the dependency is divided into two parts. In the early age both parameters are related by a power law and in the later age a linear trend can be found (trend lines A and B in Fig. 10). It should be noted that the transition between both trend lines occurs at exactly the same value of the specific surface area that was already found for the reflection loss in Fig. 9.

The dependency that was found between the compressive strength and the specific contact area seems logical since the weakest point of a microstructure built up by hydrated cement particles (see Fig. 2) is the connection between the individual particles. The specific contact area seems to be a good parameter to quantitatively describe the properties of this inter-particle connection. Since the compressive strength was measured on mortar, it can be expected that the relationship given in Fig. 10 changes when, for example, the volume ratio of sand to cement of the mortar is changed. The investigation of these relationships will be the subject of further research.

5. Conclusions

From the investigations described in this paper, the following conclusions can be drawn:

- (1) The reflection loss measured on mortar mixtures with different w/c ratios is linearly related to the

degree of hydration of the cement paste phase of the tested mortars. This relationship is valid at early ages (up to 95 h).

- (2) The reflection loss of the mortar mixtures was found to be related to the development of the volume fraction of the total and connected solid phase of the cement paste obtained from numerical simulation. The time of increase of the reflection loss and the time of the percolation threshold of the solid phase are very similar. After the percolation of the solid phase the reflection loss is governed by the volume fraction of the connected solid phase. At later ages the reflection loss develops according to the total solid phase.
- (3) The specific contact area as a parameter describing the degree of the inter-particle bonding of the cement particles was found to be uniquely related to the reflection loss measurements of the mortars independent from the w/c ratio. A bilinear relationship between the two parameters can be established.
- (4) The specific contact area of cement paste was found to be uniquely related to the compressive strength development of the tested mortars. At very early ages the parameters were found to be related by a power law. Within the first 24 h the relationship becomes linear. The transition between the trends occurs at the same value of the specific contact area that was found as the value marking the transition in the relationship between reflection loss and specific contact area.
- (5) The reflection loss measured on the Portland cement mortar mixtures is governed by the properties of the cement paste phase of the mortars.
- (6) The numerical model HYMOSTRUC3D could be successfully calibrated to experimental results and thereby used as a tool to provide reliable information about the microstructural development of the tested materials during hydration.

Acknowledgements

The research presented in this paper was funded by the Institute of Technology and Infrastructure of Northwestern University, the Center for Advanced Cement-Based Materials and the National Science Foundation (CMS-0408427). Their financial support is gratefully acknowledged.

References

- [1] T. Öztürk, J. Rapoport, J.S. Popovics, S.P. Shah, Monitoring the setting and hardening of cement-based materials with ultrasound, *Concr. Sci. Eng.* 1 (2) (1999) 83–91.
- [2] J. Rapoport, J.S. Popovics, K.V. Subramaniam, S.P. Shah, The use of ultrasound to monitor the stiffening process of Portland cement concrete with admixtures, *ACI Mater. J.* 97 (6) (2000) 675–683.
- [3] T. Voigt, Y. Akkaya, S.P. Shah, Determination of early age mortar and concrete strength by ultrasonic wave reflections, *ASCE J. Mater. Civ. Eng.* 15 (3) (2003) 247–254.

- [4] Y. Akkaya, T. Voigt, K.V. Subramaniam, S.P. Shah, Nondestructive measurement of concrete strength gain by an ultrasonic wave reflection method, *Mat. Struct.* 36 (262) (2003) 507–514.
- [5] T. Voigt, S.P. Shah, Properties of early age Portland cement mortar monitored with a shear wave reflection method, *ACI Mat J*, 101 (6).
- [6] T. Voigt, F. Dehn, S.P. Shah, Nondestructive testing of early-age concrete with an ultrasonic wave reflection method (Zerstörungsfreie Prüfung von jungem Beton mittels einer Ultraschallreflexionsmethode), *Bautechnik* 81 (6) (2004) 468–479 (in German).
- [7] K. van Breugel, “Simulation of hydration and formation of structure in hardening cement-based materials.” PhD thesis, Delft University of Technology, 1991.
- [8] G. Ye, K. van Breugel, A.L.A. Fraaij, Three-dimensional microstructure analysis of numerically simulated cementitious materials, *Cem. Concr. Res.* 33 (2) (2003) 215–222.
- [9] D.P. Bentz, Three-dimensional computer simulation of Portland cement hydration and microstructure development, *J. Am. Ceram. Soc.* 80 (1) (1997) 3–21.
- [10] E.J. Garboczi, D.P. Bentz, The effect of statistical fluctuation, finite size error, and digital resolution on the phase percolation and transport properties of the NIST cement hydration model, *Cem. Concr. Res.* 31 (10) (2001) 1501–1514.
- [11] P. Navi, C. Pignat, Three-dimensional characterization of the pore structure of a simulated cement paste, *Cem. Concr. Res.* 29 (4) (1999) 507–514.
- [12] H.M. Jennings, A model for the microstructure of calcium silicate hydrate in cement paste, *Cem. Concr. Res.* 30 (1) (2000) 101–116.
- [13] O. Bernard, F.-J. Ulm, E. Lemarchand, A multiscale micromechanics-hydration model for the early-age elastic properties of cement-based materials, *Cem. Concr. Res.* 33 (9) (2003) 1293–1309.
- [14] J.I. Bhatti, K.J. Reid, Use of thermal analysis in the hydration studies of a Type I Portland cement produced from mineral tailings, *Therm. Acta* 91 (1985) 95–105.
- [15] B. El-Jazairi, J.M. Illston, The hydration of cement paste using the semi-isothermal method of derivative thermogravimetry, *Cem. Concr. Res.* 10 (3) (1980) 361–366.
- [16] T.C. Powers, The nonevaporable water content of hardened Portland-cement paste—Its significance for concrete research and its method of determination, *ASTM Bull.* 158 (1949) 68–76.
- [17] H.F.W. Taylor, *Cement Chemistry*, Second Edition, Thomas Telford Publishing, London, 1997.
- [18] L. Molina, On predicting the influence of curing conditions on the degree of hydration, CBI Report 5:92, Swedish Cement and Concrete Research Institute, Stockholm, 1992.
- [19] T.C. Hansen, Physical structure of hardened cement paste. A classical approach, *Mat. Struct.* 19 (114) (1986) 423–436.
- [20] Z. Sun, G. Ye, T. Voigt, S.P. Shah, K. van Breugel, Early age properties of Portland cement pastes investigated with ultrasonic shear waves and numerical simulation, *Proc. of the RILEM International Symposium of Advances in Concrete through Science and Engineering*, Evanston, USA, 2003, on CD-ROM.
- [21] Feylessoufi, F. Cohen-Tenoudji, V. Morin, P. Richard, Early ages shrinkage mechanisms of ultra-high-performance cement-based materials, *Cem. Concr. Res.* 31 (11) (2001) 1573–1579.
- [22] ASTM C109/C109M-02, Standard test method for compressive strength of hydraulic cement mortars (using 2-in. or [50-mm] cube specimens), 2003 Book of ASTM Standards, vol. 04.01, American Society for Testing and Materials, Philadelphia, PA, 2003.